

THE ADINI FINITE ELEMENT ON LOCALLY REFINED MESHES

D. GALLISTL

ABSTRACT. This work introduces a locally refined version of the Adini finite element for the planar biharmonic equation on rectangular partitions with at most one hanging node per edge. If global continuity of the discrete functions is enforced, for such method there is some freedom in assigning the normal derivative degree of freedom at the hanging nodes. It is proven that the convergence order h^2 known for regular solutions and regular partitions is lost for any such choice, and that assigning an average of the normal derivatives at the neighbouring regular vertices is the only choice that achieves a super-linear order, namely $h^{3/2}$ on uniformly refined meshes. On adaptive meshes, the method behaves like a first-order scheme. Furthermore, the reliability and efficiency of an explicit residual-based error estimator are shown up to the best approximation of the Hessian by certain piecewise polynomial functions.

1. INTRODUCTION AND MAIN RESULTS

While Galerkin methods enjoy the error bound from Céa's lemma and, therefore, local mesh refinement with nested spaces does not increase the approximation error, in nonconforming discretizations—a popular choice for the biharmonic equation—local refinement of the mesh resolution may potentially disimprove the situation. The main purpose of this work is an analysis of this phenomenon in a model situation. The Adini finite element method (FEM) is one of the earliest methods for numerically solving the biharmonic equation [1, 6]. It is a standard four-noded rectangular element in the engineering literature, and therein also referred to as Adini–Clough–Melosh element [13]. Given a rectangular partition \mathcal{T} of the underlying domain $\Omega \subseteq \mathbb{R}^2$, the shape function space for every rectangle T is the space of cubic polynomials over T enriched by the two monomials x^3y and xy^3 , where the Cartesian coordinates of a point in the plane are denoted by x, y and the mesh is assumed to be aligned with the Cartesian axes. The corresponding twelve degrees of freedom are the point evaluation of a function and the evaluation of its first-order partial derivatives in any of the four vertices. The resulting finite element, schematically shown in the mnemonic diagram of Figure 1, is easy to implement and its a priori error analysis is theoretically well understood when regular partitions are used. Regularity of a partition \mathcal{T} means that if any vertex z of an element $T \in \mathcal{T}$ belongs to some element $K \in \mathcal{T}$, it is automatically also a vertex of K . For such regular meshes it is known that the method converges at the order h^2 under uniform mesh refinement if the solution is sufficiently regular, h being the maximal mesh size [6, 12, 11]. In presence of singularities of the solution, the convergence order is significantly reduced and adaptive mesh refinement towards the singularity becomes mandatory, a case not studied so far in the literature on the Adini FEM. On rectangular partitions with bounded aspect ratio, such refinement necessarily

Date: 9th May 2025.

2020 Mathematics Subject Classification. 65N12, 65N15, 65N30.

Key words and phrases. nonconforming, hanging node, Kirchhoff plate, Serendipity.

Supported by the European Research Council (StG *DAFNE*, ID 891734).

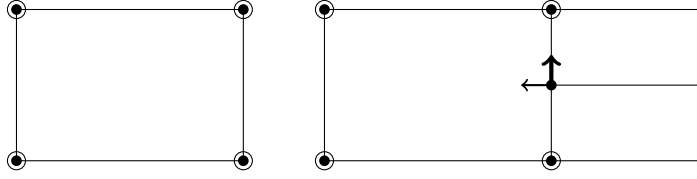


FIGURE 1. Mnemonic diagram of Adini's finite element (left); degrees of freedom at a hanging node (right).

requires elements with irregular vertices (commonly called hanging nodes), i.e., a vertex z of a rectangle T may belong to an edge of another rectangle K without being a vertex of it. The degrees of freedom attached to that hanging node are then subject to some interpolation constraint. The typical situation is displayed in Figure 1. In the case of the Adini element, the value and the derivative in the direction tangential to the edge are prescribed by the condition of the function to be globally continuous. The continuity condition for the partial derivative in the direction normal to the edge, however, is not canonically prescribed because the Adini FEM is a nonconforming method, meaning that the discrete functions are globally continuous but their gradients may be discontinuous so that the discrete functions may possibly not belong to $H^2(\Omega)$, the energy space for the biharmonic equation. Two obvious possibilities (out of many others) are: either the degree of freedom is set in such a way that it interpolates the partial derivative on the neighbouring element; or it is simply chosen as the average by linear interpolation of the partial derivatives at the neighbouring vertices determining the edge that contains the irregular vertex z in its interior. It is obvious that the latter choice cannot retain the quadratic approximation order h^2 known from the regular case because the averaging operation does not conserve cubic polynomials. However, in this work it is proven that it is the only possible choice (in the class of linear, local, and scaling-invariant couplings) that yields a superlinear order, namely $h^{3/2}$ on uniform refinements of an initial irregular mesh subjected to the condition of Definition 2.1 below.

The design of the Adini element does not involve average integrals of normal derivatives over edges as degrees of freedom, in contrast to nonconforming methods like the Morley element and others [12]. This prevents the element from passing certain patch tests, and the error analysis is more involved and relies on the choice of the shape function space, which is the same as for the lowest-order Serendipity element [3]. Consequently, a reliability proof for a residual-based error estimator has not been available [4, 8]. Furthermore, the definition of the element on meshes with hanging nodes is not straightforward because an analogue to [5, condition (A2)] is not satisfied by the normal derivative. As the first main result in this work, it is shown that the quadratic approximation order is necessarily lost in the presence of hanging nodes, showing that best-approximation results in the fashion of [10] are unavailable. It is shown that a suitable assignment of local degrees of freedom at hanging nodes can lead to $h^{3/2}$ convergence.

Theorem A (a priori error estimate). *Let $f \in L^2(\Omega)$ be such that the exact solution u to the biharmonic problem (2.1) satisfies $u \in H^4(\Omega) \cap W^{3,\infty}(\Omega)$. Let $(\mathcal{T}_h)_h$ be a sequence of uniform refinements of an initial partition that satisfies the mesh condition of Definition 2.1 and contains at least one irregular vertex. Let $u_h \in V_h$ denote the finite element solution to (2.2) where V_h is the Adini finite element space with regular assignment in the sense of Definition 3.1. The averaging assignment,*

that is the choice of V_h according to (3.2), satisfies

$$\|u - u_h\|_h \lesssim h^2 \|u\|_{H^4(\Omega)} + h \|u\|_{H^3(\cup \mathcal{T}^{\text{irr}})},$$

where $\cup \mathcal{T}^{\text{irr}}$ from (4.1) is the area covered by elements with irregular vertices. In particular, it satisfies the asymptotic bound

$$\|u - u_h\|_h \lesssim h^{3/2} (\|u\|_{H^4(\Omega)} + \|u\|_{W^{3,\infty}(\Omega)})$$

on uniformly refined meshes. For any other admissible assignment there exists a right-hand side f such that the solution $u \in C^\infty(\bar{\Omega})$ is smooth, but

$$\|u - u_h\|_h \gtrsim h.$$

Furthermore, a residual-based a posteriori error estimator is shown to be reliable and efficient up to terms that are second-order accurate on regular meshes, but only first-order on more general meshes (details on the notation follow in §2).

Theorem B (a posteriori error estimate). *Let \mathcal{T} be a partition satisfying the mesh condition of Definition 2.1 and V_h be chosen according to the averaging assignment (3.2). The solution u to the biharmonic problem (2.1) with right-hand side $f \in L^2(\Omega)$ and its Adini finite element discretization u_h from (2.2) satisfy, with $\boldsymbol{\eta}$, $\boldsymbol{\eta}(T)$ defined in (5.2), the reliability estimate*

$$\|u - u_h\|_h \lesssim \boldsymbol{\eta}$$

and local efficiency

$$\boldsymbol{\eta}(T) \lesssim \|u - u_h\|_{h,\omega_T} + \|(1 - \Pi^{\mathcal{T}})D^2u\|_T + \|h^2(1 - \Pi_0)f\|_{\omega_T}$$

for any $T \in \mathcal{T}$ with element patch ω_T and the projection $\Pi^{\mathcal{T}}$ from (5.1).

While its efficiency part is not new and can be proven with standard arguments [14], more importantly Theorem B also provides a reliability result of an a posteriori error estimator for the Adini element, which partly proves a conjecture of [4] and explains the results of their numerical experiments. Therein, the error estimator $\boldsymbol{\eta}$ (up to the additional local projection error $\|(1 - \Pi^{\mathcal{T}})D^2u\|_T$ not considered there) was experimentally observed to be an upper error bound on uniformly refined meshes. Theorem B theoretically justifies the observed convergence rates of the error estimator in [4].

The results presented here allow for two conclusions. The first one is that the Adini FEM can be used as a first-order method for resolving corner singularities and hints potential for resolving non-rectilinear (possibly curved) domains. Since the Adini shape function space is that of the Serendipity family [3], the element cannot be mapped to general quadrilaterals like trapeziums without loss of approximation quality, see the discussion in [12]. The local resolution variant of the method proposed here thus makes the Adini FEM more competitive for such situations. In some cases, it even satisfies superlinear convergence. Secondly, and perhaps more fundamentally, the analysis shows that the quadratic convergence order is necessarily lost under fairly reasonable coupling conditions at hanging nodes. This highlights that nonconforming methods do not naturally generalize to irregular partitions in absence of further structural conditions. In particular, local refinement can significantly deteriorate the approximation (as proven in Theorem A and illustrated by numerical results in §7.1), and best-approximation results analogous to those formulated in [10] do not hold in this case.

This article is organized as follows: §2 defines the necessary data structures around finite element meshes and introduces the Adini element. The assignment at hanging nodes is discussed in §3. The proof of Theorem A is provided in §4, while §5 provides the proof of Theorem B. Comments on the extension to more general boundary conditions follow in §6. Numerical experiments are shown in §7. Finally,

some important but technical estimates for discrete functions are provided in the Appendices §A–§D.

Throughout this work, standard notation on Lebesgue and Sobolev spaces is used. The L^2 norm over a measurable set ω is denoted by $\|\cdot\|_\omega$ with the convention $\|\cdot\| = \|\cdot\|_\Omega$. Polynomial functions of total resp. partial degree not greater than k are denoted by P_k resp. Q_k . The notation $a \lesssim b$ or $b \gtrsim a$ indicates an inequality $a \leq Cb$ with a constant independent of the mesh size; $a \approx b$ means $a \lesssim b \lesssim a$.

2. ADINI'S FINITE ELEMENT FOR THE BIHARMONIC EQUATION

Let $\Omega \subseteq \mathbb{R}^2$ be an open and bounded rectilinear Lipschitz polygon. Given a right-hand side $f \in L^2(\Omega)$, the biharmonic problem with clamped boundary conditions seeks $u \in H_0^2(\Omega)$ such that

$$(2.1) \quad a(u, v) = (f, v)_{L^2(\Omega)} \quad \text{for all } v \in H_0^2(\Omega),$$

where the bilinear form a is defined by

$$a(v, w) := \int_{\Omega} D^2 v : D^2 w \quad \text{for any } v, w \in H^2(\Omega)$$

and the colon $:$ denotes the Frobenius inner product of matrices.

The following notation related to a partition \mathcal{T} of Ω is used. The set of vertices (extremal points) of a rectangle is denoted by $\mathcal{V}(T)$. The set of all vertices of \mathcal{T} is denoted by \mathcal{V} . A vertex $z \in \mathcal{V}$ for which $z \in T \in \mathcal{T}$ implies $z \in \mathcal{V}(T)$, i.e., z is one of the four vertices of T , is called a regular vertex, and the set of such vertices is denoted by \mathcal{V}^{reg} . The remaining irregular vertices are denoted by $\mathcal{V}^{\text{irr}} = \mathcal{V} \setminus \mathcal{V}^{\text{reg}}$. Throughout this work, the notions *hanging node* and *irregular vertex* are used interchangeably. Any irregular $z \in \mathcal{V}^{\text{irr}}$ necessarily lies on the interior of an edge E of some rectangle T that is the convex hull of two vertices $z_1, z_2 \in \mathcal{V}(T)$, called the neighbouring vertices. In particular $z \in E = \text{conv}\{z_1, z_2\}$. Throughout this paper, we work on classes of partitions with uniformly bounded aspect ratio. The L^2 projection to piecewise (possibly discontinuous) P_k functions is denoted by Π_k . For $z \in \mathcal{V}$ and $T \in \mathcal{T}$ we define the usual patches

$$\omega_z := \text{int}(\cup\{K \in \mathcal{T} : z \in K\}) \quad \text{and} \quad \omega_T := \cup\{\omega_z : z \in \mathcal{V}(T)\}.$$

The outer unit normal of the boundary of a rectangle T is denoted by n_T . The set of all edges is denoted by \mathcal{E} . Every edge has a (globally fixed) normal vector n_E and a tangential vector t_E . If the meaning is clear from the context and there is no risk of confusion, the symbols n and t are sometimes used without index in expressions like ∂_{nn}^2 , ∂_{nt}^2 , etc. The diameter of a rectangle T and an edge E are denoted by h_T and h_E , respectively. The piecewise constant mesh-size function h is defined by $h|_T := h_T$ for any $T \in \mathcal{T}$. If the letter h is used in global expressions like $O(h^s)$ or outside norms, it denotes the maximum of the mesh size function.

The piecewise Hessian with respect to \mathcal{T} is denoted by D_h^2 , and the index h is also used to indicate piecewise partial derivatives $\partial_{j,h}$ of piecewise smooth functions. Any rectangle $T \subseteq \mathbb{R}^2$ will be assumed to be aligned with the Cartesian axes, so that any of its faces is parallel to either the x or y axis. The shape function space \mathcal{A} is that of cubic polynomials enriched by the two elements xy^3 and x^3y , written

$$\mathcal{A} = P_3 + \langle xy^3, x^3y \rangle,$$

where angle brackets denote the linear hull. If there is no risk of confusion, a polynomial function will not be distinguished from its restriction to or its extension from some subdomain of \mathbb{R}^2 throughout this work. Given a rectangle T , the twelve degrees of freedom of the Adini finite element are the point evaluations of a function and of its first partial derivatives in those vertices. A corresponding diagram is

displayed in Figure 1. Given Ω , let \mathcal{T} be a finite partition into rectangles such that the elements of T cover the domain $\cup_{T \in \mathcal{T}} T = \overline{\Omega}$ and the intersection of the interior of any two distinct elements is empty. The space of piecewise Adini functions reads

$$\mathcal{A}(\mathcal{T}) := \{v \in L^\infty(\Omega) : v|_T \in \mathcal{A} \text{ for any } T \in \mathcal{T}\}.$$

If \mathcal{T} is any such partition (with or without hanging nodes), the global finite element space with clamped boundary condition and gradient continuity at the regular vertices reads

$$\widehat{V}_h := C(\overline{\Omega}) \cap \left\{ v \in \mathcal{A}(\mathcal{T}) \left| \begin{array}{l} \nabla v \text{ is continuous in the interior regular vertices of } \mathcal{T} \\ v \text{ and } \nabla v \text{ vanish on the boundary vertices of } \mathcal{T} \end{array} \right. \right\}.$$

The continuity requirement shows that \widehat{V}_h is spanned by $\mathcal{A}(\mathcal{T})$ functions that are continuous in all vertices, with continuous gradient in all regular vertices and with continuous tangential derivative at irregular vertices ('tangential' referring to the edge containing the hanging node). No condition is made on the normal derivative at such vertex although it is a local degree of freedom for the finite element. For regular partitions, $V_h = \widehat{V}_h$ is the standard Adini finite element space known from the literature. In this case it is known that $V_h \subseteq C(\overline{\Omega})$ is a space of continuous functions with possibly discontinuous piecewise derivatives. This means that V_h is a subspace of the Sobolev space $H_0^1(\Omega)$ but in general not a subspace of the energy space $H_0^2(\Omega)$ for the biharmonic problem, whence it is referred to as nonconforming. If the partition contains irregular vertices, a subspace $V_h \subseteq \widehat{V}_h$ needs to be considered such that the discrete problem is well posed. The Adini finite element discretization is based on the discrete bilinear form

$$a_h(v, w) := \int_{\Omega} D_h^2 v : D_h^2 w \quad \text{for any } v, w \in H_0^2(\Omega) + \widehat{V}_h,$$

where D_h^2 denotes the piecewise Hessian with respect to \mathcal{T} . Under the admissibility condition of Definition 3.1 below, V_h is such that a_h is positive definite over V_h . The seminorm induced by a_h and denoted by $\|\cdot\|_h$ is a norm on V_h under this assumption. The discretization seeks $u_h \in V_h$ such that

$$(2.2) \quad a_h(u_h, v_h) = (f, v_h)_{L^2(\Omega)} \quad \text{for all } v_h \in V_h.$$

It is well known that, for regular partitions, this is a convergent method on a sequence of uniformly refined rectangles with maximal mesh size h . The error bound shown in [11] states the quadratic order

$$\|u - u_h\|_h \lesssim h^2 \|u\|_{H^4(\Omega)}.$$

In the general case of possibly nonconvex domains, the assumed regularity is unrealistic, and local mesh refinement is required for resolving singularities or the domain geometry. For rectangular and shape-regular partitions, this necessarily leads to hanging nodes. The main question is which continuity properties to enforce at hanging nodes in the definition of V_h in order to obtain a method with good convergence properties. Here, we focus on 1-irregular partitions with a maximum of one hanging node per edge.

Definition 2.1 (mesh condition). We say that \mathcal{T} satisfies the mesh condition if for any irregular $z \in \mathcal{V}^{\text{irr}}$ (1) its neighbouring vertices z_1, z_2 are regular and (2) any pair $z_1, z_2 \in \mathcal{V}^{\text{reg}}$ of regular vertices forming an edge hosts at most one irregular vertex, i.e., $\text{card}(\text{conv}\{z_1, z_2\} \cap \mathcal{V}^{\text{irr}}) \leq 1$.

This condition means that every edge containing an irregular vertex in its interior connects two regular vertices and does not contain any further irregular vertex. Figure 2 shows some configurations excluded by this condition, while typical admissible configurations are displayed in Figure 3 or Figure 6. Let \mathcal{T} be a partition satisfying

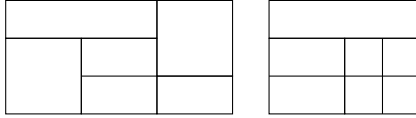


FIGURE 2. Mesh configurations excluded by Definition 2.1. Left: some neighbouring vertices are irregular. Right: an edge contains more than one irregular vertex.

the condition of Definition 2.1. Such partitions allow for simple Q_1 interpolation. For any function v over $\bar{\Omega}$ that is continuous in the regular vertices \mathcal{V}^{reg} , the interpolation Qv is the globally continuous and piecewise bilinear function defined by assigning the nodal value of v at the regular vertices and, for irregular vertices, the value of the affine interpolation between the values at the two neighbouring vertices. That is, Qv is defined by

$$(2.3) \quad Qv(z) = \begin{cases} v(z) & \text{if } z \in \mathcal{V}^{\text{reg}} \\ (\lambda_1 + \lambda_2)^{-1}(\lambda_2 v(z_1) + \lambda_1 v(z_2)) & \text{if } z \in \mathcal{V}^{\text{irr}} \text{ has neighbours } z_1, z_2 \end{cases}$$

with the weights $\lambda_j := |z - z_j|$, $j = 1, 2$. The approximation properties of Q are discussed in Lemma B.1 in §B of the appendix.

The Adini space V_h over \mathcal{T} is assumed to be a subspace of \widehat{V}_h from §2. This fixes the point values in all vertices, the gradient values in regular vertices, and, for any irregular vertex z , the partial derivative in tangential direction of the edge E containing z . It does not fix the partial derivative at z in the direction normal to E . We will now discuss possible choices in the next section.

3. CONTINUITY CONDITIONS AT HANGING NODES

For a 1-irregular partition \mathcal{T} , an interior edge with a hanging node $z \in \mathcal{V}^{\text{irr}}$ will be shared by three rectangles: one rectangle T for which z is not a vertex, $z \notin \mathcal{V}(T)$, and two rectangles K_1, K_2 which have z as a vertex, see Figure 3. The local degrees of freedom related to z cannot be a global degree of freedom. Instead, a choice for the value of the function and its gradient at z has to be made. For global continuity, it is necessary that v and the tangential derivative of v are continuous at z . The only freedom that is left is the choice of the derivative normal to T at z . Any sensible choice must guarantee approximation and consistency. We ask the assignment of the normal derivative to be linear, local, and scaling-invariant:

Definition 3.1 (admissible assignment). Let $z \in \mathcal{V}^{\text{irr}}$ be an irregular vertex. There exist exactly three elements $T, K_1, K_2 \in \mathcal{T}$ that contain z , where z is a vertex of K_1, K_2 and belongs to the interior of an edge E of T (see Figure 3) with normal vector n_E . A function $v \in \widehat{V}_h$ is said to satisfy an admissible assignment at z if

$$\frac{\partial v|_{K_1}}{\partial n_E}(z) = \frac{\partial v|_{K_2}}{\partial n_E}(z) = L(v|_T)$$

for a linear operator L that (1) is invariant under relabelling coordinates and under linear scaling (homothety), i.e., if \hat{v} is defined by $x \mapsto v(\lambda x)$ for a positive real λ , then $L\hat{v} = \lambda Lv$, and (2) conserves the normal derivative at z for all quadratic polynomials. A subspace $V_h \subseteq \widehat{V}_h$ is said to satisfy an admissible assignment if any $v_h \in V_h$ satisfies an admissible assignment at every $z \in \mathcal{V}^{\text{irr}}$ and if the kernel of a_h over V_h equals $\{0\}$.

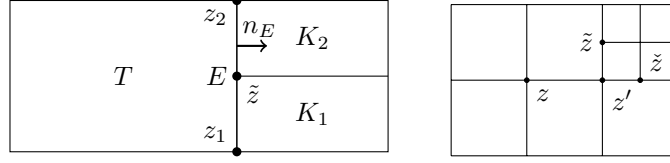


FIGURE 3. Left: Configuration with a hanging node \tilde{z} . Right: Mesh configuration with a regular vertex z and exactly one irregular vertex \tilde{z} on $\partial\omega_z$.

Throughout this work, we assume that V_h is a linear subspace of \widehat{V}_h satisfying an admissible assignment; in particular a_h is a scalar product on V_h . Then problem (2.2) has a unique solution $u_h \in V_h$, and the classical a priori error bound [3, Lemma 10.1.7] known as Berger–Scott–Strang lemma states that

$$(3.1) \quad \max\{A, B\} \leq \|u - u_h\|_h \leq A + B$$

for the approximation and consistency errors

$$A := \inf_{v_h \in V_h} \|u - v_h\|_h \quad \text{and} \quad B := \sup_{v_h \in V_h \setminus \{0\}} a_h(u - u_h, v_h) / \|v_h\|_h.$$

For the method to converge at rate h^s it is necessary that both A and B decrease at least at that rate. A priori error estimates are usually formulated on sequences of uniformly refined meshes. Here, uniform refinement means that every rectangle is split into four equal sub-rectangles by connecting the midpoints of opposite edges with straight lines. If this refinement process is started from an initial 1-irregular partition, eventually the partition will contain regular vertices z with exactly one irregular vertex on the boundary of their vertex patch ω_z , as displayed in Figure 3.

We say a method is $O(h^s)$ if there exists a constant $C > 0$ such that $\|u - u_h\|_h \leq Ch^s(\|u\|_{H^4(\Omega)} + \|u\|_{W^{3,\infty}(\Omega)})$ provided the norm of u on the right-hand side is finite. According to the assignment rule of Definition 3.1, the space V_h is spanned by global basis functions related to the degrees of freedom at regular vertices. The following lemma states that necessary for convergence better than $O(h)$ is that certain basis functions related to regular vertices are continued by 0 by the admissible assignment.

Lemma 3.2. *Let \mathcal{T} be a 1-irregular partition such that there exists a regular vertex $z \in \mathcal{V}^{\text{reg}}$ with $\partial\omega_z \subseteq \Omega$ and exactly one irregular vertex $\tilde{z} \in \mathcal{V}^{\text{irr}}$ on the boundary of its vertex patch and without irregular vertices inside ω_z (see Figure 3). Let $E \subseteq \partial\omega_z$ denote the edge containing \tilde{z} and let z' denote the vertex forming an edge with z and being neighbour to \tilde{z} . Let $\varphi = \varphi_{z,\alpha}$ with $|\alpha| \leq 1$ denote the Adini basis functions with respect to function or derivative evaluation at z (defined in §A of the appendix) with respect to the multiindex α . If $\partial_{n_E} \varphi_{z,\alpha}(\tilde{z})$ follows an admissible assignment and $\varphi_{z,\alpha}$ is not continued by 0 outside ω_z , then there exists an f such that the solution u belongs to $H^4(\Omega) \cap W^{3,\infty}(\Omega)$, but $\|u - u_h\|_h \geq c_1 h_E - c_2 h_E^2$ with positive numbers c_1, c_2 independent of the mesh size. The same holds true if the admissible assignment depends nontrivially on the function value at z' .*

Proof. Let u be the solution to (2.1) and assume $u \in H^4(\Omega)$. Consider the consistency term B from the a priori result (3.1). Due to (2.2) it satisfies

$$B \geq \|\varphi\|_h^{-1} \left(a_h(u, \varphi) - \int_{\Omega} f \varphi \right).$$

We follow the notation of Figure 3 and denote by K_1, K_2 the rectangles with $\tilde{z} \in \mathcal{V}(K_1) \cap \mathcal{V}(K_2)$. Clearly, due to the locality in Definition 3.1, φ vanishes

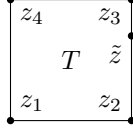


FIGURE 4. Notation for the reference rectangle used in Lemma 3.3.

identically outside $\omega_z \cup K_1 \cup K_2$. We assume that φ is not continued by 0 outside ω_z and therefore we have with some nonzero real number c that

$$\varphi|_{K_1 \cup K_2} = c\psi$$

where ψ is the (local) basis function with $\psi = \varphi_{\tilde{z}, \beta}$ on $K_1 \cup K_2$ with $\beta \neq 0$ parallel to n_E (see §A of the appendix for the notation around the Adini basis functions). From standard scaling we thus have

$$\|D_h^2 \varphi\|_{L^2(K_1 \cup K_2)} \approx |c| \quad \text{and} \quad \|D_h^2 \varphi\|_{L^2(\omega_z)} \approx h_E^{|\alpha|-1}.$$

The scaling invariance of Definition 3.1 implies $|c| \approx h_E^{|\alpha|-1}$ so that

$$\|\varphi\|_h \approx h_E^{|\alpha|-1}.$$

Thus,

$$B \gtrsim h_E^{1-|\alpha|} \left(\int_{\omega_z \cup K_1 \cup K_2} D^2 u : D_h^2 \varphi - \int_{\Omega} f \varphi \right).$$

From scaling of φ we also have

$$\left| \int_{\Omega} f \varphi \right| \lesssim h_E^{1+|\alpha|} \|f\|_{L^2(\Omega)}.$$

Further, it can be computed (see Lemma A.4 in §A of the appendix) that

$$\int_{\omega_z} p \partial_{jk,h}^2 \varphi = 0 \quad \text{for any affine } p \in P_1 \text{ and any } j, k = 1, 2.$$

Standard estimates thus show that $|\int_{\omega_z} D^2 u : D_h^2 \varphi|$ is bounded by a constant times $h_E^2 \|u\|_{H^4(\Omega)} \|\varphi\|_h$. We thus obtain constants C_1, C_2 such that

$$B \geq -C_1 h_E^2 (\|u\|_{H^4(\Omega)} + \|f\|_{L^2(\Omega)}) + C_2 h_E^{1-|\alpha|} \int_{K_1 \cup K_2} D^2 u : D_h^2 \varphi.$$

Now, by the above requirements, $\varphi|_{K_1 \cup K_2}$ must coincide with $c\psi$. We explicitly compute with Lemma A.6 that

$$\int_{K_1 \cup K_2} D_h^2 \varphi = c h_E \begin{bmatrix} \gamma_1 & 0 \\ 0 & \gamma_2 \end{bmatrix} \quad \text{with } \gamma_1 \gamma_2 = 0 \text{ and } \gamma_1 + \gamma_2 \neq 0.$$

Without loss of generality, assume that $c\gamma_1 > 0$. Then, if $D^2 u$ is uniformly positive definite in a neighbourhood of $K_1 \cup K_2$, we get the asserted lower bound for B from the scaling of $|c|$. Such u can be easily obtained by multiplying the function $(x^2 + y^2)/2$ with a smooth cutoff function which is constant 1 in a neighbourhood of $K_1 \cup K_2$, so that the Hessian of u equals the unit matrix in that region.

In the case that the assignment for the normal derivative at \tilde{z} depends nontrivially on the function value at z' , consider the global basis function $\varphi = \varphi_{z', (0,0)}$. Since, by Lemma A.5, the diagonal derivatives $\partial_{jj,h}^2 \varphi$ are L^2 orthogonal to affine functions, and since by the tangential continuity of φ the mixed derivative $\partial_{xy,h}^2 \varphi$ can be integrated by parts against $\partial_{xy}^2 u$ without interface jumps, we have as above that $|\int_{\Omega} D^2 u : D_h^2 \varphi| \lesssim h_E^2 \|u\|_{H^4(\Omega)} \|\varphi\|_h$. The lower bound then follows with an argument analogous to the one above. \square

The foregoing Lemma 3.2 has the following implication. For $|\alpha| \leq 1$, the lower bound in the proof is better than linear only if $c = 0$. If $\partial_{n_E} \varphi_{z,\alpha}(\tilde{z})$ follows an admissible assignment and the method convergences like $O(h^s)$ with $s > 1$ on quasi-uniform meshes, then necessarily $\varphi_{z,\alpha}$ is continued by 0 outside ω_z . Likewise, the normal-derivative degree of freedom must not be coupled with the point evaluation at a neighbouring vertex. For the assignment operator L , using the notation for a reference element as displayed in Figure 4 with hanging node z , the lemma states that L must map the basis functions $\varphi_{z_1,\alpha}$ and $\varphi_{z_4,\alpha}$ with $|\alpha| \leq 1$ to zero. The next result shows that the averaging is the only potentially superlinear admissible refinement rule that preserves quadratic polynomials. Recall the Adini basis functions from §A of the appendix.

Lemma 3.3. *Consider the reference square $(-1,1)^2$ from Figure 4 with vertices z_1, \dots, z_4 in counterclockwise enumeration starting with $z_1 = (-1,-1)$. Further denote $\tilde{z} = (r,0)$ with $-1 < r < 1$. The only linear admissible (in the sense of Definition 3.1) map $L : \mathcal{A} \rightarrow \mathbb{R}$ $L\varphi_{z_2,(0,0)} = 0$ as well as*

$$L\varphi_{z_j,\beta} = 0 \text{ for } j = 1,4 \text{ and } |\beta| \leq 1, \quad \text{and} \quad \partial_x p(\tilde{z}) = Lp \quad \text{for all } p \in P_2$$

is the averaging

$$Lp := \frac{1}{2}((1-r)\partial_x p(z_2) + (1+r)\partial_x p(z_3)).$$

The space P_3 of cubic polynomials is not invariant under such assignment.

Proof. Since $P_3 \subseteq \mathcal{A}$, any cubic polynomial can be represented in the Adini basis as

$$p = \sum_{j=1}^4 \sum_{|\alpha| \leq 1} \partial^\alpha p(z_j) \varphi_{z_j,\alpha}.$$

From linearity of L and the assumptions, we obtain

$$Lp = \sum_{j=2,3} \sum_{|\alpha| \leq 1} \partial^\alpha p(z_j) L\varphi_{z_j,\alpha}.$$

Plugging in the polynomials $q = (x-1)y$ and $\tilde{q} = (x-1)$ and equating with the x -derivative at \tilde{z} then yields

$$r = Lq = -L\varphi_{z_2,(1,0)} + L\varphi_{z_3,(1,0)} \quad \text{and} \quad 1 = L\tilde{q} = L\varphi_{z_2,(1,0)} + L\varphi_{z_3,(1,0)}$$

and therefore $L\varphi_{z_2,(1,0)} = (1-r)/2$ and $L\varphi_{z_3,(1,0)} = (1+r)/2$. Similarly, the polynomials 1 (the constant) and $(y^2-1)/2$ lead to

$$0 = L\varphi_{z_2,(0,0)} + L\varphi_{z_3,(0,0)} \quad \text{and} \quad 0 = -L\varphi_{z_2,(0,1)} + L\varphi_{z_3,(0,1)},$$

which implies $L\varphi_{z_2,(0,0)} = -L\varphi_{z_3,(0,0)}$ and $L\varphi_{z_2,(0,1)} = L\varphi_{z_3,(0,1)}$. Using the assumption $L\varphi_{z_2,(0,0)} = 0$ thus shows $L\varphi_{z_2,(0,0)} = 0 = L\varphi_{z_3,(0,0)}$. Plugging in the polynomial y further yields

$$0 = L\varphi_{z_2,(0,1)} + L\varphi_{z_3,(0,1)},$$

which results in $L\varphi_{z_2,(0,1)} = 0 = L\varphi_{z_3,(0,1)}$.

Altogether, the only choice for an admissible map L is the asserted averaging. It remains to check that this choice cannot preserve all cubic polynomials. For the choice $p = (1-y^2)(1-x)$, we see that $\partial_x p$ vanishes at all vertices. Hence, we have $Lp = 0$ but $\partial_x p(\tilde{z}) = -(1-r^2) \neq 0$. \square

The foregoing two Lemmas 3.2–3.3 show that the averaging assignment is the only candidate that potentially achieves superlinear convergence, which in particular proves the lower error bound stated in Theorem A. Hence, the choice proposed

here is to assign the average of the normal derivatives at the neighbouring vertices: The global Adini finite element space is defined by

$$(3.2) \quad V_h := \left\{ v \in \widehat{V}_h : Q\nabla v \text{ is continuous at } \mathcal{V}^{\text{irr}} \right\}$$

with the bilinear interpolation operator Q defined in (2.3).

4. ANALYSIS OF THE CONSISTENCY ERROR, PROOF OF THEOREM A

Throughout this section, the choice of V_h is fixed through the averaging rule (3.2). On any T we introduce local coordinates

$$\xi(x, y) = h_x^{-1}(x - m) \quad \text{and} \quad \eta(x, y) = h_y^{-1}(y - m)$$

ranging from -1 to 1 , where m is the midpoint of T and h_x, h_y are the half widths in x, y direction, respectively. By Q we denote the globally continuous and piecewise bilinear interpolation from (2.3). By the assignment of the hanging node value as in (3.2), the expression $Q\partial_x w$ is well defined for any $w \in V_h$. We note the following fact, which is essentially contained in [11].

Lemma 4.1. *Let T be a rectangle with E an edge orthogonal to the x -axis. Then any $w \in \mathcal{A}$ satisfies*

$$(1 - Q)\partial_x w|_E = -\frac{h_y^3}{3}\partial_{xyyy}^4 w(\eta^3 - \eta) + \frac{h_y^2}{2}\partial_{xyy}^3 w(\eta^2 - 1).$$

Proof. We express the monomials of the Adini space in terms of ξ, η . It is obvious that $\partial_x P_2$ and $\partial_x \langle \xi^2 \eta, \eta^3 \rangle$ belong to Q_1 . Further $\partial_x \langle \xi^3, \xi^3 \eta \rangle$ consists of functions that are linear in η and thus are interpolated exactly by Q on E . Therefore, the only two remaining monomials are $\xi \eta^2, \xi \eta^3$, and

$$(1 - Q)\partial_x w|_E = (1 - Q)\partial_x (a\xi \eta^3 + b\xi \eta^2)|_E$$

with real coefficients a, b . The chain rule reveals $\partial_x \xi = h_x^{-1}, \partial_y \eta = h_y^{-1}$. Taking derivatives of w and comparing coefficients shows that

$$\partial_{xyyy}^4 w = \frac{6}{h_x h_y^3} a \quad \text{and} \quad \partial_{xyy}^3 w = \frac{1}{h_x h_y^2} (6a\eta + 2b),$$

which leads to

$$a = \frac{h_x h_y^3}{6} \partial_{xyyy}^4 w \quad \text{and} \quad b = \frac{h_x h_y^2}{2} \partial_{xyy}^3 w - 3a\eta.$$

A direct computation of derivatives and interpolation leads to

$$(1 - Q)\partial_x (a\xi \eta^3 + b\xi \eta^2)|_E = h_x^{-1} (a(\eta^3 - \eta) + b(\eta^2 - 1)).$$

Inserting the values for a and b in this formula reveals the asserted identity. \square

The previous lemma will be essential for bounding the consistency term in the next lemma. We denote

$$(4.1) \quad \mathcal{T}^{\text{reg}} := \{T \in \mathcal{T} : \text{all vertices of } T \text{ are regular}\} \quad \text{and} \quad \mathcal{T}^{\text{irr}} := \mathcal{T} \setminus \mathcal{T}^{\text{reg}}.$$

Lemma 4.2. *Let the partition \mathcal{T} satisfy the condition of Definition 2.1 and let V_h be chosen according to (3.2). Let $g \in C^1(\overline{\Omega})$ be a piecewise polynomial function and $w \in V_h$. Then,*

$$\sum_{T \in \mathcal{T}} \int_{\partial T} g(1 - Q)\nabla w \cdot n_T \lesssim (\|(1 - \Pi_1)g\|_{\cup \mathcal{T}^{\text{reg}}} + \|(1 - \Pi_0)g\|_{\cup \mathcal{T}^{\text{irr}}}) \|D_h^2 w\|.$$

The constant hidden in the notation \lesssim may depend on the polynomial degree of g .

Proof. We consider the edges orthogonal to the x or y axis separately. For a rectangle T we denote by n_x the x component of the outer unit normal (left -1 , right 1 , top and bottom 0). Fix any T with local coordinates (ξ, η) . For $(1 - Q)\partial_x w$ we use the expression from Lemma 4.1 and the fundamental theorem of calculus so that

$$(4.2) \quad \int_{\partial T} g(1 - Q)\partial_x w n_x = -\frac{h_y^3}{3} \int_T \partial_x g \partial_{xyyy}^4 w (\eta^3 - \eta) + \frac{h_y^2}{2} \int_T \partial_x g \partial_{xyy}^3 w (\eta^2 - 1),$$

where it has been used that the fourth and third derivatives of w appearing in Lemma 4.1 do not depend on x . Since the function $\eta^3 - \eta$ has vanishing average over T , and since the fourth derivative of w is constant, we can use orthogonality to constants and the Cauchy inequality for the first term on the right-hand side of (4.2) to see

$$(4.3a) \quad -\frac{h_y^3}{3} \int_T \partial_x g \partial_{xyyy}^4 w (\eta^3 - \eta) \leq \frac{h_y^3}{3} \|(1 - \Pi_0)\partial_x g\|_T \|\partial_{xyyy}^4 w\|_T \|\eta^3 - \eta\|_{L^\infty(T)}.$$

With the inverse estimate and $0 \leq \eta \leq 1$ we obtain that this is bounded by some constant times

$$(4.3b) \quad h_y \|(1 - \Pi_0)\partial_x g\|_T \|\partial_{xy}^2 w\|_T.$$

Next, consider the second term of (4.2). With the global bilinear interpolation Q from (2.3) we obtain with the abbreviation $e := w - Qw$ (note that $\partial_{xyy}^3 w$ and $\partial_{xyy}^3 e$ coincide) and integration by parts with respect to y that

$$\frac{h_y^2}{2} \int_T \partial_x g (\eta^2 - 1) \partial_{xyy}^3 w = -\frac{h_y^2}{2} \int_T \partial_{xyy}^2 g (\eta^2 - 1) \partial_{xy}^2 e - h_y \int_T \partial_x g \eta \partial_{xy}^2 e.$$

Again, with integration by parts with respect to x ,

$$-h_y \int_T \partial_x g \eta \partial_{xy}^2 e = h_y \int_T \partial_{xx}^2 g \eta \partial_y e - h_y \int_{\partial T} \partial_x g \eta \partial_y e n_x.$$

Integrating by parts along any edge E parallel to the y axis with end points z_-, z_+ reveals

$$-h_y \int_E \partial_x g \eta \partial_y e = h_y \int_E \partial_{xy}^2 g \eta e + \int_E \partial_x g e - h_y ((\partial_x g e)(z_+) + (\partial_x g e)(z_-)).$$

Combining the three foregoing displayed identities yields

$$(4.4) \quad \begin{aligned} & \frac{h_y^2}{2} \int_T \partial_x g (\eta^2 - 1) \partial_{xyy}^3 w \\ &= -\frac{h_y^2}{2} \int_T \partial_{xyy}^2 g (\eta^2 - 1) \partial_{xy}^2 e + h_y \int_T \partial_{xx}^2 g \eta \partial_y e + h_y \int_{\partial T} \partial_{xy}^2 g \eta e n_x + R(T) \end{aligned}$$

with

$$R(T) := \int_{\partial T} \partial_x g e n_x - \sum_{z \in \mathcal{V}(T)} h_y n_x (\partial_x g e)(z).$$

We note that the inverse inequality implies for any second-order derivative ∂_{jk}^2 of the polynomial $g|_T$ that

$$\|\partial_{jk}^2 g\|_T \lesssim h_T^{-1} \|(1 - \Pi_0)\partial_j g\|_T.$$

The combination of (4.2)–(4.4) with this estimate, the bound $0 \leq \eta \leq 1$, trace and inverse inequalities, and the approximation and stability properties of Q from Lemma B.1, lead to

$$\int_{\partial T} g(1 - Q)\partial_x w n_x \lesssim h_T \|(1 - \Pi_0)\partial_x g\|_T \|D_h^2 w\|_{\omega_T} + R(T).$$

Of course we have $h_T \|(1 - \Pi_0) \partial_x g\|_T \lesssim \|(1 - \Pi_1) g\|_T$ for the polynomial $g|_T$. Considering the sum over all T , since $\partial_x g$ and e are globally continuous and since e vanishes on $\partial\Omega$, we have that

$$\sum_{T \in \mathcal{T}} \int_{\partial T} \partial_x g e n_x = 0.$$

We further note that $e(z) = 0$ for every regular vertex z . Therefore,

$$\sum_{T \in \mathcal{T}} R(T) \lesssim \sum_{T \in \mathcal{T}} \sum_{z \in \mathcal{V}(T) \cap \mathcal{V}^{\text{irr}}} |h_T (\partial_x g e)(z)|.$$

Given $z \in V(T) \cap \mathcal{V}^{\text{irr}}$, trace and inverse estimates show with the stability properties of Q from Lemma B.1 that

$$|h_y (\partial_x g e)(z)| \lesssim \|(1 - \Pi_0) g\|_T \|D_h^2 w\|_{\omega_T}.$$

Combining the above estimates results in the asserted estimate with n_T replaced by n_x . An analogous argument shows the same bound for n_T replaced by n_y , so that eventually the full assertion follows. \square

Proof of Theorem A. The abstract a priori error estimate (3.1) shows that the error is bounded by $A + B$. We start by bounding A . Let $I_h u$ denote the standard Adini interpolation of u described in §D of the appendix. On any element $T \in \mathcal{T}^{\text{reg}}$ with regular vertices, the standard interpolation bound shows $\|D_h^2(u - I_h u)\|_T \lesssim h_T^2 \|D^4 u\|_T$. If $T \in \mathcal{T}^{\text{irr}}$ contains an irregular vertex, I_h preserves quadratic functions and therefore the standard interpolation bound shows $\|D_h^2(u - I_h u)\|_T \lesssim h_T \|D^3 u\|_T$. Altogether,

$$A^2 \leq \|D_h^2(u - I_h u)\|_{\cup \mathcal{T}^{\text{reg}}}^2 + \|D_h^2(u - I_h u)\|_{\cup \mathcal{T}^{\text{irr}}}^2 \lesssim h^4 \|u\|_{H^4(\cup \mathcal{T}^{\text{reg}})}^2 + h^2 \|u\|_{H^3(\cup \mathcal{T}^{\text{irr}})}^2.$$

For bounding the term B , consider any $v_h \in V_h$ with $\|v_h\|_h = 1$. Then, the solution property of u_h , integration by parts, and $\Delta^2 u = f$ show

$$a(u - u_h, v_h) = \sum_{T \in \mathcal{T}} \int_{\partial T} \partial_{nn}^2 u \nabla v_h \cdot n_T = \sum_{T \in \mathcal{T}} \int_{\partial T} \partial_{nn}^2 u (1 - Q) \nabla v_h \cdot n_T$$

because $Q \nabla v_h$ is continuous and vanishes on the boundary. Let $\mathbf{g} := \mathcal{J} D^2 u \in [C^1(\bar{\Omega})]^{2 \times 2}$ denote the (component-wise) BFS averaging of $D^2 u$ defined in §C. Adding and subtracting \mathbf{g} in the above identity results in

$$a_h(u - u_h, v_h) = \sum_{T \in \mathcal{T}} \int_{\partial T} (\partial_{nn}^2 u - \mathbf{g}_{nn})(1 - Q) \nabla v_h \cdot n_T + \sum_{T \in \mathcal{T}} \int_{\partial T} \mathbf{g}_{nn} (1 - Q) \nabla v_h \cdot n_T.$$

Trace inequalities and the approximation and discrete stability properties of Q and \mathcal{J} from Lemma B.1 and Lemma C.1 bound the first sum on the right-hand side as follows

$$\sum_{T \in \mathcal{T}} \int_{\partial T} (\partial_{nn}^2 u - \mathbf{g}_{nn})(1 - Q) \nabla v_h \cdot n_T \lesssim h^2 \|u\|_{H^4(\Omega)} \|v_h\|_h.$$

The second term in the above split is bounded with the help of Lemma 4.2. A piecewise use of Poincaré's inequality and Lemma C.1 then conclude the proof of the first stated upper error bound in Theorem A. Under uniform mesh refinement, the area covered by elements with irregular vertices scales like

$$\text{meas}(\cup \mathcal{T}^{\text{irr}}) \lesssim h.$$

The first error bound and the assumed L^∞ bound on the third derivatives thus imply

$$\|u - u_h\|_h^2 \lesssim h^4 \|u\|_{H^4(\cup \mathcal{T}^{\text{reg}})}^2 + h^3 \|u\|_{W^{3,\infty}(\cup \mathcal{T}^{\text{irr}})}^2$$

and thus the second stated upper error bound. The stated lower error bound follows from Lemmas 3.2–3.3.

5. A POSTERIORI ERROR ESTIMATE, PROOF OF THEOREM B

We define the projection operator $\Pi^{\mathcal{T}}$ by

$$(5.1) \quad \Pi^{\mathcal{T}}v|_T := \begin{cases} \Pi_1 v|_T & \text{if } T \in \mathcal{T}^{\text{reg}} \\ \Pi_0 v|_T & \text{if } T \in \mathcal{T}^{\text{irr}}. \end{cases}$$

Any edge is equipped with a fixed normal vector n_E and tangential vector t_E . The jump across E is denoted by $[\cdot]_E$; for boundary edges, $[\cdot]_E$ denotes the trace.

For any $T \in \mathcal{T}$ define the local error estimator contribution by

$$(5.2a) \quad \boldsymbol{\eta}^2(T) = h_T^4 \|f\|_T^2 + \sum_{j=1}^3 \sum_{E \in \mathcal{E}(T)} \kappa_j^E h_T^{2j-3} \left\| \left[\frac{\partial^j u_h}{\partial n_E^j} \right]_E \right\|_E^2 + \|(1 - \Pi^{\mathcal{T}})D^2 u_h\|_T^2,$$

where $\mathcal{E}(T)$ is the set of edges of T and

$$\kappa_j^E = \begin{cases} 0 & \text{if } j \geq 2 \text{ and } E \subseteq \partial\Omega, \\ 1 & \text{otherwise} \end{cases}$$

is introduced for excluding boundary edges from the sums when second- and third-order normal derivatives of u_h are considered. Define the total error estimator

$$(5.2b) \quad \boldsymbol{\eta} = \left(\sum_{T \in \mathcal{T}} \boldsymbol{\eta}^2(T) \right)^{1/2}.$$

Proof of Theorem B. As in [4], the error is orthogonally split as follows

$$\|u - u_h\|_h^2 = \left[\sup_{\varphi \in H_0^2(\Omega) \setminus \{0\}} \frac{a_h(u - u_h, \varphi)}{\|\varphi\|_h} \right]^2 + \min_{v \in H_0^2(\Omega)} \|u_h - v\|_h^2.$$

Since the second term on the right-hand side is directly bounded by $\boldsymbol{\eta}^2$ after plugging in the BFS averaging $v = \mathcal{J}_0 u_h$ with zero boundary conditions from §C and using the bound from Lemma C.1 and inverse estimates, it remains to bound the first term. Let $\varphi \in H_0^2(\Omega)$ with $\|\varphi\|_h = 1$ and denote by $I_h \mathcal{J} \varphi$ its Adini quasi-interpolation from §D of the appendix and abbreviate $\hat{\varphi} := \varphi - I_h \mathcal{J} \varphi$. Equation 2.1 and the discrete solution property (2.2) yield

$$a_h(u - u_h, \varphi) = \int_{\Omega} f \hat{\varphi} - a_h(u_h, \hat{\varphi}).$$

The first term on the right-hand side is readily bounded by $\boldsymbol{\eta}$ through (D.1). For the analysis of the second term, consider its contribution on any element T . Two integrations by parts reveal

$$\int_T D^2 u_h : D^2 \hat{\varphi} = \int_{\partial T} \partial_{nn}^2 u_h \partial_n \hat{\varphi} + \int_{\partial T} \partial_{nt}^2 u_h \partial_t \hat{\varphi} - \int_{\partial T} (\text{div } D^2 u_h) \cdot n \hat{\varphi}.$$

Summing over all elements and noting that $\hat{\varphi}$ and so $\partial_t \hat{\varphi}$ is continuous, we obtain

$$a_h(u_h, \hat{\varphi}) = \sum_{T \in \mathcal{T}} \int_{\partial T} \partial_{nn}^2 u_h \partial_n \hat{\varphi} + \sum_{E \in \mathcal{E}} \left(\int_E [\partial_{nt}^2 u_h]_E \partial_t \hat{\varphi} - \int_E [\text{div } D^2 u_h]_E \cdot n_E \hat{\varphi} \right).$$

Standard estimates [14] with (D.1) bound the last two terms by $\boldsymbol{\eta}$. In particular, by $\hat{\varphi} = \partial_t \hat{\varphi} = 0$ on $\partial\Omega$ the boundary edges do not contribute to the sum. For the analysis of the first sum on the right-hand side, denote by $\mathbf{g} := \mathcal{J} D_h^2 u_h$ the

component-wise BFS averaging of the piecewise Hessian from §C. We have with $\varphi \in H_0^2(\Omega)$ and the continuity of \mathbf{g} and $Q\nabla I_h \mathcal{J}\varphi$ that

$$\sum_{T \in \mathcal{T}} \int_{\partial T} \partial_{nn}^2 u_h \partial_n \hat{\varphi} = \sum_{T \in \mathcal{T}} \left(\int_{\partial T} (\partial_{nn}^2 u_h - \mathbf{g}_{nn}) \partial_n \hat{\varphi} + \int_{\partial T} \mathbf{g}_{nn} (Q - 1) \nabla I_h \mathcal{J}\varphi \cdot n_T \right).$$

The trace and inverse inequalities and Lemma 4.2 show that this is bounded by a constant times

$$\sum_{j=1,2} (\|\partial_{jj}^2 u_h - \mathbf{g}_{jj}\| + \|(1 - \Pi^{\mathcal{J}}) \mathbf{g}_{jj}\|),$$

where we used (D.1) and $\|D_h^2 \varphi\| = 1$. Since, obviously,

$$\|(1 - \Pi^{\mathcal{J}}) \mathbf{g}_{jj}\| \leq \|(1 - \Pi^{\mathcal{J}}) \partial_{jj}^2 u_h\| + \|\mathbf{g}_{jj} - \partial_{jj}^2 u_h\|$$

we eventually have

$$\sum_{T \in \mathcal{T}} \int_{\partial T} \partial_{nn}^2 u_h \partial_n \hat{\varphi} \lesssim (\|D_h^2 u_h - \mathbf{g}\| + \|(1 - \Pi^{\mathcal{J}}) D^2 u_h\|).$$

The last term is part of (and thus bounded by) $\boldsymbol{\eta}$. The bound of the first term follows from Lemma C.1. This concludes the proof of reliability. The efficiency follows from known arguments [14, 4].

6. EXTENSION TO OTHER BOUNDARY CONDITIONS

This section explains how the proofs shown for clamped boundary conditions in the foregoing sections extend to other boundary conditions, which are relevant in plate bending, flow problems, or phase separation models. As the prototypical situation in linear plate theory, we consider a disjoint partition of $\partial\Omega$ as $\partial\Omega = \Gamma_C \cup \Gamma_S \cup \Gamma_F$ in clamped (Γ_C), simply supported (Γ_S), and free (Γ_F) part and consider the energy space

$$V = \{v \in H^2(\Omega) : v = 0 \text{ on } \Gamma_C \cup \Gamma_S \text{ and } \partial_n v = 0 \text{ on } \Gamma_C\}$$

instead of $H_0^2(\Omega)$ from prior sections where $\partial\Omega = \Gamma_C$ was assumed. The variational problem is then to find $u \in V$ solving (2.1) with $H_0^2(\Omega)$ replaced by V . The strong form reads

$$\Delta^2 u = f \text{ in } \Omega \quad \text{and} \quad u = 0 \text{ on } \Gamma_C \cup \Gamma_S \text{ and } \partial_n u = 0 \text{ on } \Gamma_C$$

with the natural boundary conditions

$$\partial_{nn}^2 u = 0 \text{ on } \Gamma_S \cup \Gamma_F \text{ and } \partial_n (\partial_{nn}^2 u + 2\partial_{tt}^2 u) = 0 \text{ on } \Gamma_F.$$

Here n denotes the outer unit vector on $\partial\Omega$ and $t = (-n_2, n_1)$ is a unit tangent vector. The problem is well posed provided the boundary configuration is such that V does not contain affine functions. For the discretization with the Adini FEM we assume that the boundary edges match with the decomposition of the boundary and that Γ_C and $\Gamma_C \cup \Gamma_S$ are relatively closed sets and replace the definition of \widehat{V}_h from §2 by

$$\widehat{V}_h := C(\overline{\Omega}) \cap \left\{ v \in \mathcal{A}(\mathcal{T}) \left| \begin{array}{l} \nabla v \text{ is continuous in the interior regular vertices of } \mathcal{T} \\ v \text{ and } \nabla v \cdot t \text{ vanish on the vertices of } \Gamma_C \cup \Gamma_S \\ \nabla v \cdot n \text{ vanishes on the vertices of } \Gamma_C \end{array} \right. \right\}.$$

The Adini finite element space is then V_h from (3.2) where the modified version of \widehat{V}_h is used. The discrete problem seeks $u_h \in V_h$ solving (2.2) where again this modified V_h is used.

The results of §3 as well as Lemma 4.1 hold without modifications. The error bound of Lemma 4.2 holds with $\cup \mathcal{T}^{\text{irr}}$ replaced by

$$(\cup \mathcal{T}^{\text{irr}}) \cup \{T \in \mathcal{T} : T \cap \Gamma_F \neq \emptyset\}$$

on the right-hand side. In the proof, only the analysis of the term $\sum_{T \in \mathcal{T}} R(T)$ requires modifications. Indeed, since e therein vanishes on $\Gamma_C \cup \Gamma_S$, but not necessarily on Γ_F , we have

$$\sum_{T \in \mathcal{T}} \int_{\partial T} \partial_x g e n_x = \sum_{E \subseteq \bar{\Gamma}_F} \int_E \partial_x g e n_x,$$

where the sum on the right-hand side is over all edges contained in the closure of Γ_F . This term is then bounded with trace and inverse inequalities and leads to the increased integration domain of $(1 - \Pi_0)g$ mentioned above. Theorem A applies to this situation as well, again with the same replacement of $\cup \mathcal{T}^{\text{irr}}$ stemming from the use of Lemma 4.2 in the proof. Note that in the proof of Theorem A the product $\partial_{nn}^2 u Q \nabla v_h \cdot n$ still vanishes on the whole boundary due to the natural boundary condition satisfied by u . In particular, the asymptotic convergence rate $h^{3/2}$ remains true because the area covered by the element touching the free boundary Γ_F scales like h .

For the extension of Theorem B, we need to modify the projection $\Pi^{\mathcal{J}}$ from (5.1) in so far as $\Pi^{\mathcal{J}} v|_T$ should equal $\Pi_0 v|_T$ also on the elements having an edge on $\bar{\Gamma}_F$. With this definition, the error estimator contribution $\boldsymbol{\eta}^2(T)$ is defined as

$$\begin{aligned} \boldsymbol{\eta}^2(T) &= h_T^4 \|f\|_T^2 + \sum_{j=1}^3 \sum_{E \in \mathcal{E}(T)} \kappa_j^E h_T^{2j-3} \left\| \left[\frac{\partial^j u_h}{\partial n_E^j} \right]_E \right\|_E^2 + \|(1 - \Pi^{\mathcal{J}})D^2 u_h\|_T^2 \\ &+ \sum_{\substack{E \in \mathcal{E}(T) \\ E \subseteq \bar{\Gamma}_F}} h_T^3 \left\| \left[\partial_{n_E} \left(\frac{\partial^2 u_h}{\partial n_E^2} + 2 \frac{\partial^2 u_h}{\partial t_E^2} \right) \right]_E \right\|_E^2, \end{aligned}$$

where

$$\kappa_j^E = \begin{cases} 0 & \text{if } j \in \{2, 3\} \text{ and } E \subseteq \bar{\Gamma}_C, \\ 0 & \text{if } j \in \{1, 3\} \text{ and } E \subseteq \bar{\Gamma}_S \cup \bar{\Gamma}_F, \\ 1 & \text{otherwise} \end{cases}$$

such that the residuals of the natural boundary conditions on Γ_S and Γ_F and of the essential boundary conditions on Γ_C and Γ_S are adequately included. With these modifications, Theorem B holds for the situation of general boundary as well. In the proof, $H_0^2(\Omega)$ needs to be replaced by V , the BFS averaging \mathcal{J} needs to be defined accordingly so that essential boundary conditions correspond to Γ_C and Γ_S (see [7, Proposition 2.5] for a similar operator). The same applies to the Adini interpolation I_h . With these adaptations, the proof of Theorem B is very similar to the one given in §5. As a major modification, on the edges of Γ_F , the prior statement $\hat{\varphi} = \partial_t \hat{\varphi} = 0$ does not hold. Instead, after integration by parts in tangential direction, the additional residual enters the error estimator.

7. NUMERICAL RESULTS

7.1. Illustration of Theorem A on quasi-uniform meshes. We start by numerically illustrating the upper and lower a priori error bounds in an elementary setting with the square $\Omega = (-1, 1)^2$ and f such that the exact solution is given by the biquartic polynomial $u = -(x^4 - 2x^2 + 1)(y^4 - 2y^2 + 1)$. We consider a regular coarse initial partition consisting of four congruent squares, and sequences of meshes following two refinement variants. In the first variant (Variant I), the coarse mesh is uniformly refined once, and thereafter only one element containing the point $(0, 0)$ is refined, resulting in an irregular partition. From this third mesh on, again uniform refinements are performed. In the second variant (Variant II), five uniform refinements of the initial mesh are performed before the seventh mesh is generated

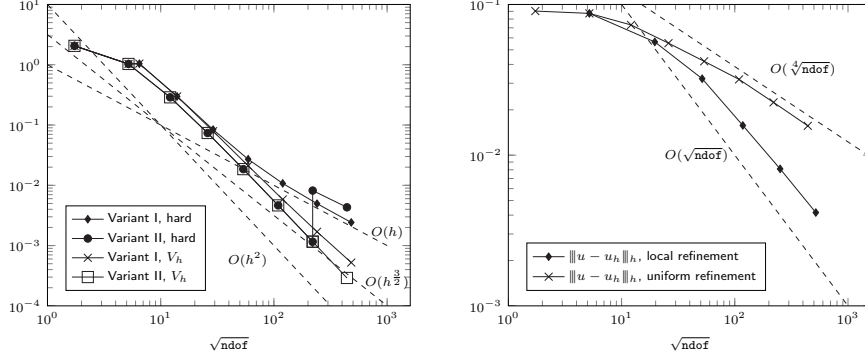


FIGURE 5. Left: Numerical illustration of Theorem A with the errors $\|u - u_h\|_h$ for a smooth u on the unit square, setting of §7.1. Right: Convergence history for the disk domain from §7.2.

by refining only one element containing $(0, 0)$. After that, the refinements are again uniform.

For the sake of a consistent presentation, in convergence history plots of this work, the horizontal axis displays the squareroot of the number of degrees of freedom ndof . For these quasi-uniform meshes in this example, that quantity is proportional to h , the parameter used in Theorem A. Starting from the third mesh in the sequence, the partitions of Variant I are irregular. Theorem A predicts the error to decrease as $h^{3/2}$ for V_h as in (3.2) and not better than h for any other choice. Up to the seventh mesh, the partitions of Variant II are uniform, so that Theorem A states errors of the order h^2 on these regular partitions. After the local refinement, the partitions are irregular, and Theorem A predicts the error for V_h as in (3.2) to gradually deteriorate to $h^{3/2}$, while any other method must immediately deteriorate from $O(h^2)$ to $O(h)$.

Figure 5 (left) displays the convergence history of the $\|\cdot\|_h$ error with respect to the squareroot of the number of degrees of freedom ndof (the dashed lines showing the asymptotic rates are labelled with powers of the proportional parameter h used in Theorem A). Two assignments are compared: the assignment (3.2), abbreviated by V_h in the legend, and the enforcement of strong continuity of the normal derivative in irregular vertices, abbreviated by ‘hard’. The results are as expected: for Variant I, the ‘hard’ interpolation results in convergence $O(h)$, while the method (3.2) reaches the predicted $O(h^{3/2})$. For Variant II, as soon as a single element is refined and, thus, the partition becomes irregular, the ‘hard’ interpolation method immediately deteriorates to $O(h)$.

7.2. Approximation of a curvilinear domain. As an example for local resolution of a curved boundary, consider Ω as the unit disk with $f = 1$ and the exact solution given by $u(x, y) = 2^{-6}(x^2 + y^2 - 1)^2$ and discretization by the averaging assignment (3.2). For the domain approximation, we consider a partition of the square $(-1, 1)^2$ where all degrees of freedom related to vertices outside Ω are set to zero. On a sequence of uniformly refined meshes this results in convergence of order $h^{1/2}$ as can be seen in the convergence history of Figure 5 (right). In a locally refined variant, from the j -th uniform refinement of the background mesh, the actual partition is generated by repeating j times: mark all elements that touch the boundary $\partial\Omega$ for local refinement and generate the smallest 1-irregular partition where the marked elements are refined. Figure 6 (left) shows an instance of

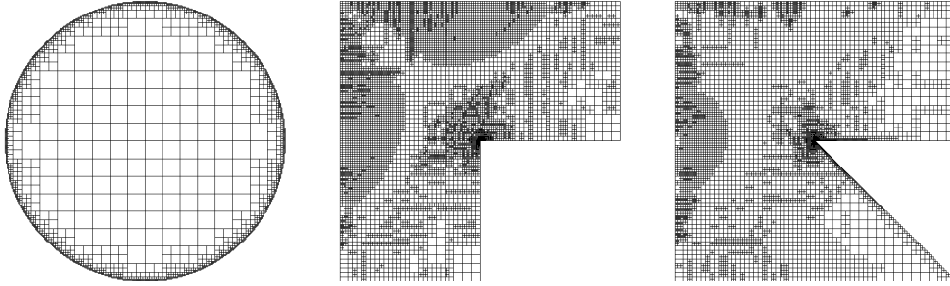


FIGURE 6. Left: Locally resolved disk, 13 875 degrees of freedom. Middle: Adaptive mesh of the L-domain, 37 119 degrees of freedom, level 17. Right: Adaptive mesh of the cusp domain, 32 130 degrees of freedom, level 19.

such a mesh; and the convergence history showing that this local refinement variant improves the convergence order to $\sqrt{\text{ndof}}$.

7.3. Adaptive mesh refinement. In this experiment, we consider the error estimator $\boldsymbol{\eta}$ with its local contributions $\boldsymbol{\eta}(T)$ as a refinement indicator in an adaptive mesh-refinement algorithm with Dörfler marking and bulk parameter chosen as $1/2$ in a standard adaptivity loop [14]. We consider the L-shaped domain $\Omega = (-1, 1)^2 \setminus ([0, 1] \times [-1, 0])$. With $\alpha = 0.5444837\dots$ and $\omega = 3\pi/2$, the exact singular solution from [9, p. 107] reads in polar coordinates as

$$(7.1) \quad u(r, \theta) = (r^2 \cos^2 \theta - 1)^2 (r^2 \sin^2 \theta - 1)^2 r^{1+\alpha} g(\theta),$$

with the function

$$g(\theta) = \left(\frac{s_-(\omega)}{\alpha - 1} - \frac{s_+(\omega)}{\alpha + 1} \right) (c_-(\theta) - c_+(\theta)) - \left(\frac{s_-(\theta)}{\alpha - 1} - \frac{s_+(\theta)}{\alpha + 1} \right) (c_-(\omega) - c_+(\omega))$$

and the abbreviations $s_{\pm}(z) = \sin((\alpha \pm 1)z)$ and $c_{\pm}(z) = \cos((\alpha \pm 1)z)$. The convergence history with respect to the squareroot of the number of degrees of freedom (ndof) is displayed in Figure 7 (left). As expected, uniform mesh refinement converges with the suboptimal rate dictated by α . Adaptive mesh refinement with the averaging assignment (3.2) recovers first-order convergence, while the variant enforcing the ‘hard’ interpolation constraint performs poorly (on the same adaptive meshes) because its error is bounded from below by certain elements of large mesh size (Theorem A), see the adaptive mesh displayed in Figure 6 (middle).

7.4. Approximation of a non-rectilinear domain. As an example for adaptive resolution of a non-rectilinear domain, consider the corner domain $\Omega = (-1, 1)^2 \setminus \text{conv}\{(0, 0), (1, -1), (1, 0)\}$ with exact solution given by (7.1) for the parameters $\alpha = 0.50500969\dots$ and $\omega = 7\pi/4$. The line with angle $7\pi/4$ describes the non-rectilinear part of the boundary. We use an interior approximation with rectangles and add on elements T touching the boundary the local error estimator contribution $h_T^2 \boldsymbol{\eta}^2$ to $\boldsymbol{\eta}^2(T)$ in the marking process. This accounts for the error by the boundary approximation. Figure 7 (right) shows the convergence history. As in the previous example, adaptive mesh refinement improves the reduced convergence observed on uniform meshes. An adaptive mesh is displayed in Figure 6 (right).

7.5. Mixed boundary conditions. In this example, the generalization of the method and the a posteriori error estimator from §6 to more general boundary

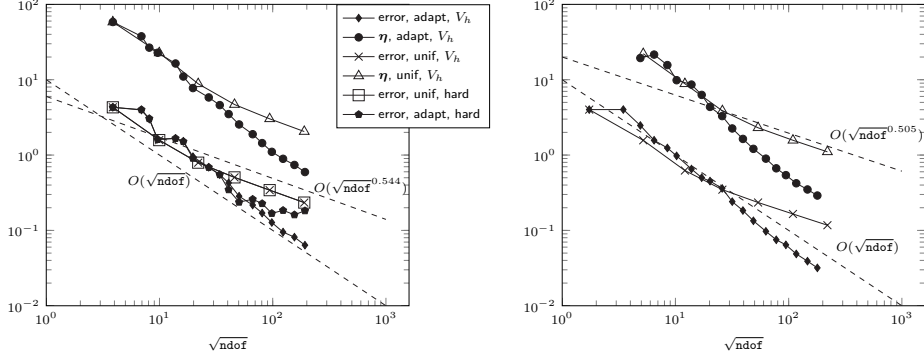


FIGURE 7. Convergence history of the error $\|u - u_h\|_h$ and the estimator η for the L-shaped (left) and the cusp (right) domain from §§7.3–7.4.

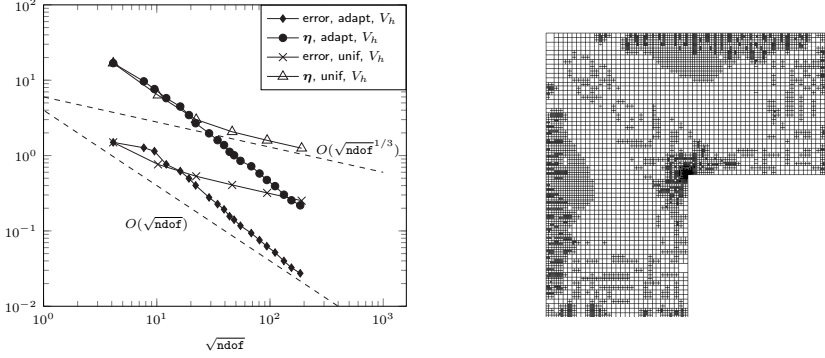


FIGURE 8. Convergence history of the error $\|u - u_h\|_h$ and the estimator η for the L-shaped domain with mixed boundary conditions from §7.5 (left). Adaptive mesh of this problem with 34 224 degrees of freedom, level 20 (right).

conditions are applied. On the L-shaped domain, the following mixed configuration in simply supported and clamped parts is chosen

$$\Gamma_S = (\{0\} \times (-1, 0]) \cup ([0, 1) \times \{0\}) \quad \text{and} \quad \Gamma_C = \Omega \setminus \Gamma_S.$$

and the right-hand f side is chosen according to the exact solution

$$u(x, y) = r^{4/3} \sin(4\theta/3)(1 - x^2)^2(1 - y^2)^2$$

with polar coordinates r, θ as functions of x, y . This function belongs to $H^{7/3-\nu}(\Omega)$ for every $\nu > 0$ but not for $\nu = 0$ and it is known [2] that this is the generic singularity for the simply supported boundary condition at an opening angle $3\pi/2$. The convergence history of uniform and adaptive mesh refinement and an adaptive mesh are displayed Figure 8. As expected, uniform mesh refinement cannot converge with a rate higher than $1/3$, whereas the adaptive version leads to errors decreasing like $\sqrt{\text{ndof}}$.

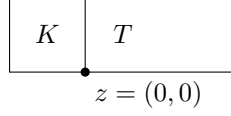


FIGURE 9. Vertex $z = (0, 0)$ shared by T , K with common edge lying on the y axis.

APPENDIX A. PROPERTIES OF THE ADINI BASIS FUNCTIONS

The Adini basis function $\varphi_{z,\alpha} \in \widehat{V}_h$ with respect to a regular vertex $z \in \mathcal{V}^{\text{reg}}$ and a multiindex $\alpha \in \{(0, 0), (1, 0), (0, 1)\}$ satisfies

$$\partial^\beta \varphi_{z,\alpha}(\tilde{z}) = \delta_{z,\tilde{z}} \delta_{\alpha,\beta} \quad \text{for all } \tilde{z} \in \mathcal{V}^{\text{reg}} \text{ and } \beta \in \{(0, 0), (1, 0), (0, 1)\}$$

with the Kronecker δ . This uniquely defines $\varphi_{z,\alpha}$ on regular partitions. On partitions with irregular vertices, it uniquely defines $\varphi_{z,\alpha}$ on elements T with $\mathcal{V}(T) \subseteq \mathcal{V}^{\text{reg}}$, that is, on elements with only regular vertices.

In what follows we consider two rectangles T , K sharing an edge lying on the y axis, with one vertex being $z = (0, 0)$, as shown in Figure 9. The ratio of the x -widths of T , K is denoted by

$$\rho = \text{diam}_x(T) / \text{diam}_x(K).$$

The following results are formulated in the coordinates (x, y) if T, K are considered. If only T is considered, the usual local coordinates ξ, η are employed.

Lemma A.1. *In the configuration of Figure 9, $\varphi = \varphi_{z,(0,0)}$ satisfies*

$$(a) \int_T q \partial_{xx}^2 \varphi = 0, \quad (b) \int_{T \cup K} x \partial_{xx}^2 \varphi = 0, \quad (c) \int_{T \cup K} q \partial_{xy}^2 \varphi = 0$$

for any integrable function $q = q(y)$ depending only on y .

Proof. For the proof of (a), we use local coordinates ξ, η , write $\hat{q}(\eta) = q(y)$, and observe that φ vanishes identically at $\eta = 1$ and $\partial_{xx}^2 \varphi$ is bilinear, so that there exists a first-order polynomial $p_1 = p_1(\xi)$ such that $\partial_{xx}^2 \varphi = (1 - \eta)p_1(\xi)$. Since $\partial_x \varphi$ vanishes at all vertices of T , considering $\eta = -1$ with the fundamental theorem of calculus shows that

$$\int_{-1}^1 \partial_{xx}^2 p_1(\xi) d\xi = 0.$$

The original integral then reads

$$\int_T \hat{q}(\eta) \partial_{xx}^2 \varphi = h_x h_y \int_{-1}^1 \hat{q}(\eta) (1 - \eta) d\eta \int_{-1}^1 \partial_{xx}^2 p_1(\xi) d\xi = 0.$$

For the proof of (b), we use the symmetry $\varphi|_K(x, y) = \varphi|_T(-\rho x, y)$ for $x \in K$. By the change of variables $\hat{x} = -\rho x$ we have for the (undirected) volume integrals that

$$\int_K x \partial_{xx}^2 \varphi(x, y) dx dy = \int_T \frac{-\hat{x}}{\rho} \partial_{xx}^2 \varphi(\hat{x}, y) |-\rho^{-1}| d\hat{x} dy = - \int_T \hat{x} \partial_{\hat{x}\hat{x}}^2 \varphi(\hat{x}, y) d\hat{x} dy.$$

This implies (b). An analogous computation shows (c). \square

Lemma A.2. *In the configuration of Figure 9, $\varphi = \varphi_{z,(1,0)}$ satisfies*

$$(a) \int_T x \partial_{xx}^2 \varphi = 0, \quad (b) \int_T q \partial_{xy}^2 \varphi = 0, \quad (c) \int_{T \cup K} q \partial_{xx}^2 \varphi = 0$$

for any integrable function $q = q(y)$ depending only on y .

Proof. Since φ vanishes on all sides apart from $\{\eta = -1\}$, it contains the linear factors $(\eta - 1)(\xi + 1)(\xi - 1)$. Since $\varphi|_T \in \mathcal{A}$, for $\partial_x \varphi$ to vanish on the two endpoints of the face $\xi = 1$, an additional factor $(\xi - 1)$ is necessary. The presence of the resulting factor $(\xi - 1)^2$ shows that φ_x vanishes on the whole face $\xi = 1$. Integration by parts then reads

$$\int_T x \partial_{xx}^2 \varphi = - \int_T \partial_x \varphi.$$

This equals zero because φ has zero boundary conditions, which proves (a). For the proof of (b), integration by parts with respect to y shows

$$h_y \int_T \hat{q}(\eta) \partial_{xy}^2 \varphi = h_y \sum_{\sigma=\pm 1} \int_{\{\eta=\sigma\}} \sigma \hat{q}(\sigma) \partial_x \varphi - \int_T \partial_y \hat{q}(\eta) \partial_x \varphi.$$

Integration by parts with respect to x shows that all these integrals vanish because φ vanishes identically on the edges parallel to the y axis. This shows (b). We note the symmetry $\varphi|_K(x, y) = -\rho^{-1} \varphi|_T(-\rho x, y)$. A computation analogous to that of the proof of (b) in Lemma A.1 thus proves (c). \square

Lemma A.3. *In the configuration of Figure 9, $\varphi = \varphi_{z,(0,1)}$ satisfies*

$$\int_{T \cup K} q \partial_{xy}^2 \varphi = 0 \quad \text{and} \quad \partial_{xx}^2 \varphi = 0$$

for any integrable function $q = q(y)$ depending only on y .

Proof. With the symmetry $\varphi|_K(x, y) = \varphi|_T(-\rho x, y)$, an argument similar to that of the proof of (b) in Lemma A.1 proves the first identity. Since the bilinear function $\partial_{xx}^2 \varphi$ vanishes on the faces parallel to the x axis, we have $\partial_{xx}^2 \varphi = 0$, which is the second asserted identity. \square

Lemma A.4. *Let z be a regular interior vertex whose patch ω_z does not contain irregular vertices. Any*

$$\varphi \in \{\varphi_{z,(0,0)}, \varphi_{z,(1,0)}, \varphi_{z,(0,1)}\}$$

out of the three global Adini basis functions related to z satisfies

$$\int_{\omega_z} p \partial_{jk}^2 \varphi dx = 0 \quad \text{for any } p \in P_1 \text{ and any pair } (j, k) \in \{1, 2\}^2.$$

Proof. The assumptions on ω_z imply that the patch is a rectangle and is formed by four rectangular elements. The assertion thus follows from carefully combining the foregoing three lemmas with suitable changes of coordinates. \square

Lemma A.5. *In the configuration of Figure 3, the global Adini basis function $\varphi = \varphi_{z',(0,0)}$ related to the point value at z' (with zero assignment for the normal derivatives at hanging nodes) satisfies*

$$\int_{\Omega} p \partial_{jj}^2 \varphi dx = 0 \quad \text{for any } p \in P_1 \text{ and any } j \in \{1, 2\}^2.$$

Proof. Let Φ denote the Adini basis function related to point evaluation at z' with respect to a coarser triangulation resulting from unifying the four smaller rectangles in Figure 3. The function φ can be written as

$$\varphi = \Phi + \sum_{|\alpha| \leq 1} c_\alpha \varphi_{\tilde{z}, \alpha} + \tilde{c} \psi_{\tilde{z}, (0,1)} + \check{c} \psi_{\tilde{z}, (1,0)}$$

for suitable coefficients $c_\alpha, \tilde{c}, \check{c}$. with $\tilde{z}, \hat{z}, \check{z}$ as in Figure 3. Lemma A.4 and Lemma A.2–A.3 (with changes of coordinates) can be applied and yield the assertion. \square

Lemma A.6. *In the configuration of Figure 9, $\varphi = \varphi_{z,(0,1)}$ satisfies*

$$\int_{T \cup K} D^2 \varphi = h_T \begin{bmatrix} 0 & 0 \\ 0 & \gamma \end{bmatrix} \quad \text{with } \gamma \approx 1.$$

Proof. Lemma A.3 shows that $\int_{T \cup K} \partial_{jk}^2 \varphi = 0$ if $\min\{j, k\} \leq 1$. From the symmetry $\varphi|_K(x, y) = \varphi|_T(-\rho x, y)$ and change of variables we further obtain

$$\int_K \partial_{yy}^2 \varphi = \rho^{-1} \int_T \partial_{yy}^2 \varphi \quad \text{and therefore} \quad \int_{T \cup K} \partial_{yy}^2 \varphi = (1 + \rho^{-1}) \int_T \partial_{yy}^2 \varphi.$$

Since φ vanishes on all edges of T apart from $\{\xi = -1\}$, an argument analogous to that of the proof of Lemma A.2 shows that $\varphi = c(\eta - 1)^2(\eta + 1)(\xi - 1)$ with some $c \approx h_y$. Then, obviously, the integral of $\partial_{yy}^2 \varphi = h_y^{-2} c(\xi - 1)(6\eta - 2)$ over T is nonzero and scales like h_T . \square

APPENDIX B. BILINEAR INTERPOLATION WITH HANGING-NODE CONSTRAINT

Given a piecewise polynomial function w that is continuous in the regular vertices of \mathcal{T} , its globally continuous and piecewise bilinear interpolation Qw is defined in (2.3).

Lemma B.1 (stability and approximation of bilinear interpolation). *Let the partition \mathcal{T} satisfy the mesh condition of Definition 2.1 and let the function w be globally continuous and piecewise polynomial with respect to \mathcal{T} . Then*

$$h_T^{-2} \|w - Qw\|_T + h_T^{-1} \|\nabla(w - Qw)\|_T + \|D^2 Qw\|_T \lesssim \|D_h^2 w\|_{\omega_T} \quad \text{for any } T \in \mathcal{T},$$
 with the element patch ω_T . The constant hidden in the notation \lesssim depends on the polynomial degree of w .

Proof. If T exclusively has regular vertices, Q is the standard bilinear interpolation on T and the result is obvious. Assume therefore that T has an irregular vertex z . Then z belongs to an edge with two neighbouring regular vertices one of them lying outside T . By the mesh condition, T must possess at least two regular vertices, so that in total there are at least three regular vertices inside $\bar{\omega}_T$ that are not collinear. At these points $w = Qw$ holds. Since the value at irregular vertices is compatible with bilinear interpolation, Q locally reproduces affine functions. The asserted result thus follows from a standard scaling argument and the finite number of possible local mesh configurations. \square

APPENDIX C. BFS AVERAGING

It is well known from the Bogner–Fox–Schmid (BFS) finite element [6] that, on any rectangle, the 16 linear functionals

$$v \mapsto \partial^\alpha v(z) \quad \text{for any vertex } z \text{ of } T \text{ and any } \alpha \in \mathfrak{B}$$

for the set $\mathfrak{B} := \{(0, 0), (1, 0), (0, 1), (1, 1)\}$ of multiindices are linear independent over Q_3 (bicubic functions). The corresponding dual BFS basis of Q_3 consists of the 16 functions $\psi_{z,\alpha}$ with

$$\partial^\beta \psi_{z,\alpha}(\tilde{z}) = \delta_{z,\tilde{z}} \delta_{\alpha,\beta} \quad \text{for all } z, \tilde{z} \in \mathcal{V}(T) \text{ and } \alpha, \beta \in \mathfrak{B}.$$

As a basic averaging operator, introduce \mathcal{M} and \mathcal{M}_0 mapping a piecewise smooth function v to a piecewise Q_3 function by assigning the mean of the above local functionals at *all vertices* (resp. all interior vertices). More precisely, for every rectangle $T \in \mathcal{T}$ and any vertex $z \in \mathcal{V}(T)$ of T , they are defined by

$$(\partial^\alpha \mathcal{M}v|_T)(z) := \overline{\sum_{\substack{K \in \mathcal{T}: \\ z \in K}} (\partial^\alpha v|_K)(z)} \quad \text{and} \quad (\partial^\alpha \mathcal{M}_0 v|_T)(z) := \begin{cases} \mathcal{M}(z) & \text{if } z \in \Omega \\ 0 & \text{if } z \in \partial\Omega \end{cases}$$

(the Σ with the bar represents the average). This function is C^1 continuous in all regular vertices, but it may be discontinuous at irregular vertices. From $\mathcal{M}v$ (resp. \mathcal{M}_0v) we construct a globally C^1 and piecewise bicubic (thus BFS) function $\mathcal{J}v$ (resp. \mathcal{J}_0v) by assigning the values of $\mathcal{M}v$ (resp. \mathcal{M}_0v) at regular vertices and by matching the values at irregular vertices by interpolation, more precisely

$$(\partial^\alpha \mathcal{J}v)(z) = \begin{cases} (\partial^\alpha \mathcal{M}v)(z) & \text{if } z \in \mathcal{V}^{\text{reg}} \\ (\partial^\alpha \mathcal{M}v|_T)(z) & \text{if } z \in \mathcal{V}^{\text{irr}} \text{ and } z \in T \setminus \mathcal{V}(T). \end{cases}$$

The definition of \mathcal{J}_0 is analogous with \mathcal{M} replaced by \mathcal{M}_0 in the above formula. In the general case that v is piecewise H^2 -regular, we overload notation and extend \mathcal{J} by defining $\mathcal{J}v := \mathcal{J}\Pi_{Q_3}v$ for the L^2 projection Π_{Q_3} to piecewise bicubic functions. As in prior sections we denote by $[\cdot]_E$ the jump across an edge E .

Lemma C.1. *Let \mathcal{T} be a partition satisfying the mesh condition of Definition 2.1. Any piecewise Q_3 (bicubic) function $v \in L^2(\Omega)$ satisfies*

$$\|v - \mathcal{J}_0v\|^2 \lesssim \sum_{E \in \mathcal{E}} (h_E \| [v]_E \|_E^2 + h_E^3 \| [\nabla v]_E \cdot n_E \|_E^2).$$

If $v \in H^2(\Omega)$, we have

$$\|h^{-2}(v - \mathcal{J}v)\| + \|h^{-1}\nabla(v - \mathcal{J}v)\| + \|D^2\mathcal{J}v\| \lesssim \|D^2v\|.$$

Proof. Let v be piecewise bicubic. Let $T \in \mathcal{T}$ and $z \in \mathcal{V}(T)$ be a vertex of T . Standard techniques [3, 4] reveal for the basic averaging operator \mathcal{M}_0 that

$$\sum_{\alpha \in \mathfrak{B}} h_T^{1+|\alpha|} |\partial^\alpha (v - \mathcal{M}_0v)(z)| \lesssim \left(\sum_{E \in \mathcal{E}: z \in E} (h_T \| [v]_E \|_E^2 + h_T^3 \| [\nabla v]_E \cdot n_E \|_E^2) \right)^{1/2}.$$

If z is a regular vertex, the same estimate obviously holds for \mathcal{M}_0 replaced by \mathcal{J}_0 . If z is an irregular vertex and K is the element with $z \in K \setminus \mathcal{V}(K)$, then $(\partial^\alpha \mathcal{J}_0v)(z)$ is defined by interpolation from information of \mathcal{M}_0v in the neighbouring vertices z_1, z_2 ; and a scaling argument shows that

$$\partial^\alpha (v - \mathcal{J}_0v)|_T(z) = (\partial^\alpha v|_T - \partial^\alpha \mathcal{M}_0v|_K)(z) \lesssim \sum_{j=1}^2 \sum_{\beta \in \mathfrak{B}} h_T^{|\beta| - |\alpha|} |\partial^\beta (v - \mathcal{M}_0v)|_{T_j}(z_j)|,$$

where T_1, T_2 are the two rectangles with $\{z, z_j\} \subseteq \mathcal{V}(T_j)$ (one of them being T). Since the expansion of $v - \mathcal{J}_0v$ on T in terms of the BFS basis functions and the scaling of the latter read

$$(v - \mathcal{J}_0v)|_T = \sum_{\alpha \in \mathfrak{B}} \sum_{z \in \mathcal{V}(T)} \partial^\alpha (v - \mathcal{J}_0v)(z) \psi_{\alpha, z} \quad \text{and} \quad \|\psi_{\alpha, z}\|_T \lesssim h_T^{1+|\alpha|},$$

a direct computation with the triangle inequality and the above estimates at the vertices and the local equivalence $h_T \approx h_E$ reveal that

$$\|v - \mathcal{J}_0v\|_T \lesssim \left(\sum_{z \in \mathcal{V}(T)} \sum_{E \in \mathcal{E}: z \in E} (h_E \| [v]_E \|_E^2 + h_E^3 \| [\nabla v]_E \cdot n_E \|_E^2) \right)^{1/2}.$$

This and the finite overlap of the element patches proves the first stated estimate for \mathcal{J}_0 . An analogous argument shows that the same upper bound is valid for $\|v - \mathcal{J}v\|^2$. The second stated estimate follows from combining this bound with local trace inequalities and standard estimates for the piecewise L^2 projection. \square

We remark that in the upper bound of $\|v - \mathcal{J}v\|^2$ mentioned in the proof of the foregoing lemma, the boundary edges can be dropped, which is, however, not made use of in this work.

APPENDIX D. ADINI QUASI-INTERPOLATION

We denote by I_h the standard Adini interpolation with zero boundary data acting on a sufficiently smooth function $w \in C^1(\overline{\Omega})$ as

$$I_h w|_T = \sum_{z \in \mathcal{V}(T) \cap \Omega} \sum_{|\alpha| \leq 1} \partial^\alpha w(z) \varphi_{z,\alpha} \quad \text{for any } T \in \mathcal{T}$$

with $\varphi_{z,\alpha}$ defined in §A. Let $v \in H_0^2(\Omega)$. We define the Adini quasi-interpolation $I_h \mathcal{J}v \in V_h$, where \mathcal{J} is the BFS averaging from §C. With Lemma C.1 and standard discrete estimates we obtain

$$(D.1) \quad \|h^{-2}(v - I_h \mathcal{J}v)\| + \|h^{-1}\nabla(v - I_h \mathcal{J}v)\| + \|D_h^2 I_h \mathcal{J}v\| \lesssim \|D^2 v\|.$$

REFERENCES

- [1] A. Adini and R. W. Clough. Analysis of plate bending by the finite element method. *NSF report*, G-7337, 1961.
- [2] H. Blum and R. Rannacher. On the boundary value problem of the biharmonic operator on domains with angular corners. *Math. Methods Appl. Sci.*, 2(4):556–581, 1980.
- [3] S. C. Brenner and L. R. Scott. *The Mathematical Theory of Finite Element Methods*, volume 15 of *Texts in Applied Mathematics*. Springer, New York, third edition, 2008.
- [4] C. Carstensen, D. Gallistl, and J. Hu. A posteriori error estimates for nonconforming finite element methods for fourth-order problems on rectangles. *Numer. Math.*, 124(2):309–335, 2013.
- [5] C. Carstensen and J. Hu. Hanging nodes in the unifying theory of a posteriori finite element error control. *J. Comput. Math.*, 27(2-3):215–236, 2009.
- [6] P. G. Ciarlet. *The Finite Element Method for Elliptic Problems*, volume 4 of *Studies in Mathematics and its Applications*. North-Holland, Amsterdam, 1978.
- [7] D. Gallistl. Morley finite element method for the eigenvalues of the biharmonic operator. *IMA J. Numer. Anal.*, 35(4):1779–1811, 2015.
- [8] D. Gallistl and S. Tian. A posteriori error estimates for nonconforming discretizations of singularly perturbed biharmonic operators. *SMAI J. Comput. Math.*, 10:355–372, 2024.
- [9] P. Grisvard. *Singularities in Boundary Value Problems*, volume 22 of *Recherches en Mathématiques Appliquées*. Masson, Paris, 1992.
- [10] T. Gudi. A new error analysis for discontinuous finite element methods for linear elliptic problems. *Math. Comp.*, 79(272):2169–2189, 2010.
- [11] J. Hu, X. Yang, and S. Zhang. Capacity of the Adini element for biharmonic equations. *J. Sci. Comput.*, 69(3):1366–1383, 2016.
- [12] P. Lascaux and P. Lesaint. Some nonconforming finite elements for the plate bending problem. *Rev. Française Automat. Informat. Recherche Operationnelle*, 9(R-1):9–53, 1975.
- [13] E. Oñate. *Structural analysis with the finite element method—linear statics. Volume 1. Basis and solids*. Lecture Notes on Numerical Methods in Engineering and Sciences. International Center for Numerical Methods in Engineering (CIMNE), Barcelona; Springer-Verlag, Berlin, 2009.
- [14] R. Verfürth. *A posteriori error estimation techniques for finite element methods*. Numerical Mathematics and Scientific Computation. Oxford University Press, Oxford, 2013.

INSTITUT FÜR MATHEMATIK, UNIVERSITÄT JENA, 07743 JENA, GERMANY
 Email address: dietmar.gallistl [at] uni-jena.de